BIOCHIP JOURNAL, Vol. 3, No. 1, 28-36, March 2009

Genome-wide Inspection of Chromosomal Aberrations in Microglia BV-2 Cells by Array-based Comparative Genomic Hybridization

Jin Hwan Do[1,2], Hyun Myung Ko[2], Kyoungho Suk[3], Eun Jung Park[4] & Dong-Kug Choi[2]

[1]Human Genome Center, Institute of Medical Science, University of Tokyo, 4-6-1 Shirokanedai, Minatoku, Tokyo 108-8639, Japan
[2]Bio-Food and Drug Research Center, Department of Biotechnology, Konkuk University, Chungju 380-701 Korea
[3]Department of Pharmacology, Kyungpook National University School of Medicine, Daegu 700-422, Korea
[4]Immune and Cell therapy Branch, National Cancer Center, Goyang 410-769, Korea
Correspondence and requests for materials should be addressed to D.K. Choi (choidk@kku.ac.kr)

Accepted 12 February 2009

Abstract

A growing body of evidence indicates that microglia, resident innate immune cells in the brain, play a role in host defense and tissue repair, and function as active contributors to neuron damage in neurodegenerative disease. BV-2 microglial cells immortalized by a *v-raf/v-myc* recombinant retrovirus (J2) have been widely used as a microglial cell model, but there are no reports about the chromosomal characteristics of this cell line such as a gain or loss in DNA copy number. In this report we conducted a genome-wide determination of chromosomal aberrations in BV-2 microglial cells using a high-throughput, oligonucleotide array-based comparative genomic hybridization (oaCGH) technique. A segmentation method was used to divide each chromosome into segments whose probe sequences share the same relative DNA copy number on average. The genomic location of each segment was determined using the mouse genome database (UCSC mm8, NCBI Build 36). Chromosome 4 was found to have the largest gain which located in the region of chr4 : 3377972-111570775, and chromosome 3 had the largest loss segment missing from the region of chr3 : 3445973-86952997. Segments possessing more DNA copies than normal by one copy (average of $\log_2$ ratios in segment >0.585) were observed in chromosomes 4 and 19 while segments having less DNA copies by one copy (average of $\log_2$ ratios <-1) were detected in chromosomes 1, 2, 11 and 13.

Keywords: Chromosomal aberration, Microglia, BV-2, Oligonucleotide array-CGH, Segmentation

Introduction

Microglial cells are ubiquitously distributed throughout the nervous system. They are present in large numbers representing 20% of the total glial cell population in the brain and are considered to be the resident innate immune cells of the CNS[1,2]. In the normal adult brain, microglia exhibit a characteristic ramified shape and are present in a down-regulated state as compared with other tissue macrophages. Microglial cells in the resting state demonstrate suppressed genomic activity. Microglia become activated in response to environmental alterations and brain injury, and undergoes dramatic morphological changes into activated amoeboid microglia[3,4]. Moreover, activated microglia produce a variety of inflammatory mediators and neurotoxic factors that are believed to induce neuronal cell death[3,4]. To identify functional properties of activated microglia at the celluar level and to produce a suitable model for *in vitro* studies of microglial cells, Blasi *et al*.[3] established a cell line called BV-2 that expresses many characteristics of microglial cells by the infection of a *v-raf/v-myc* carrying retrovirus (J2) to cultured microglial cells. It was reported that immortalized BV-2 cells share the secretory properties, phagocytic properties and tumor cytotoxicity of body macrophages, and furthermore exhibit the properties of activated microglia[5]. Nowadays, BV-2 cells have become one of the most widely used model cell lines for studies of activated microglial cells and of the onset or progression of neurodegenerative diseases such as Alzheimer's disease, Parkinson's disease, amyotrophic lateral sclerosis and multiple sclerosis as well as for the development of neuroprotective therapeutic agents[4,6-8].

However, variations in the genomic content, such as gains or losses in DNA copy number, of BV-2 microglial cells have never been elucidated. Chromosomal aberrations can be examined by many different techniques such as comparative genomic hybridization (CGH), fluorescent *in situ* hybridization (FISH) and

representational difference analysis (RDA)[9]. Recently, the resolution of CGH has been greatly improved by microarray technology, thus array-based CGH (aCGH) has become a successful and valuable tool for chromosome copy number analysis[10]. The aCGH platforms can be based on various sources such as BACs (Bacterial Artificial Chromosomes), YACs (Yeast Artificial Chromosomes) and PACs (P1-derived Artificial Chromosomes), cDNAs, selected PCR products and oligonucleotides[11]. In this study, we employed an oligonucleotide array CGH (oaCGH) platform from Agilent technologies (http://www.agilent.com) which consists of 60-mer oligonucleotides synthesized on arrays and enables detection of chromosomal aberrations in BV-2 cells with ~35 kb resolution. The whole-genome chromosomal characteristics of BV-2 microglial cells were identified for the first time in this study.

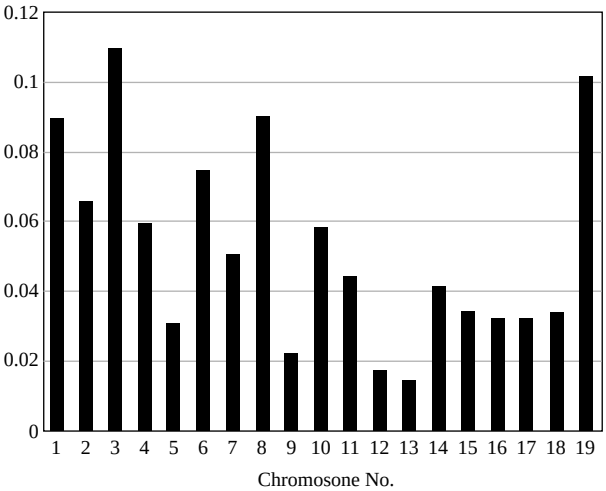

Figure 1. Distribution of 2,160 aberrant spots with $p < 0.05$ and $|\log_2 \text{ratio}| > 0.25$. The vertical axis represents the proportion of aberrant spots on each chromosome to the total number of aberrant spots.

Results and Discussion

Segmentation of oaCGH Data

Simple *t*-tests for the oaCGH data with a cross-gene error model[14] identified 3,260 spots with $p < 0.05$, which showed significantly different values from the $\log_2$ ratio of 0. When the $|\log_2 \text{ratio}| > 0.25$ was considered as the threshold for chromosomal aberration, 66% (2,160 spots) of those spots showed aberrations in DNA copy number. Chromosome 3 had the highest number of aberrations with 11% of all observed aberrations, while chromosome 13 had the least with 1% of all observed aberrations (Figure 1). Chromosome 6, in which the recombination event of the J2 virus might have occurred, also harbored 7% of all observed aberrations. Spots that exhibited a gain or loss of more than one DNA copy are shown in Table 1. The loss of genes participating in the cell cycle (*Mad2l1*) and *Metrnl* (cell differentiation) might have a close relationship with the immortalization of BV-2 cells. We surveyed the chromosome to determine the region affected by the J2 virus that led to immortalization of BV-2 cells. There are four possible regions in which the J2 virus-carrying *v-raf/v-myc* can be inserted into the mouse genome by homologous recombination: *v-raf* in chromosome 6 and X and *v-myc* in chromosome 4 and 12. However, abnormalities in DNA copy number were observed in only one of these regions, at *v-raf* in chromosome 6. More specifically, the last spot covering the *v-raf* viral oncogene 1 (chr6:115641632) had a $\log_2$ ratio of 0.74 (Figure 2), suggesting that J2 might have inserted in or near the terminal region of the *v-raf* viral oncogene 1 in chromosome 6.

In analyzing oaCGH data, gains and losses can also be defined for segments that represent homogeneous regions in the genome with the same relative copy number on average such as individual spots. We used the CGH segmentation method to identify chromosome segments or continuous sets of loci with equal ratios, except for occasional abrupt steps to a new plateau. In this way the segmentation method makes it possible to statistically assess the status of each spot in the context of its genomic neighbors. We excluded very short segments including less than three spots from our analysis. We defined segments with $|\mu_k| > \sigma$ as aberrant segments where μ_k and σ represent the mean $\log_2$ ratio of segment k and the standard deviation on chromosome including the segment, respectively. Chromosomes 1, 4, 12 and 19 have short aberrant segments of 20-100 kb while chromosomes 2, 3, 7, 8, 14, 15 and 16 contain large aberrant segment over 10 Mb (Figure 3 and Table 2). Seventy eight percent of aberrant segments with larger size than 10 Mb were loss segment. The largest loss and gain segments were observed in the region of chr3 : 3,445,973-86,952,997 (83.5 Mb) and chr3 : 87,075,657-124,604,754 (37.5 Mb), respectively. Both results of *t*-test and the CGH segmentation suggest that the chromosome 3 has most aberrations in DNA copy number. However, all spots of gain were not located in segments. This is primarily due to differences in the treatment of the data in the *t*-test versus the segmentation algorithm. The *t*-test considers aberrations and significance levels for individual spots, but the segmentation algorithm searches for continuous regions with the same level of aberration (gain or loss). Therefore, a gain spot with high ratio might be assigned to the normal

Table 1. The positions of gain/loss spots in BV-2 cells determined by single *t*-test with $p < 0.05$ ($\log_2$ ratio > 0.585 for gain spots and $\log_2$ ratio < -1 for loss spots).

Chromosome	Start position	Genes	DNA copy $\log_2$ ratio (BV-2/Normal)	Oligonucleotide No.*
1	173400488	*Cd244*	−1.1059	A_53_P131959
	175964400		1.4046	A_53_P104926
	188434889	*Rrp15*	1.2020	A_53_P141440
2	32457456	*Ak1*	1.6805	A_53_P159127
	77702452	*BC003993*	−1.4621	A_53_P132161
	77743386	*BC003993*	−1.9621	A_53_P137138
	118169037	*Srp14*	2.4694	A_53_P166342
	118376105	*Pak6*	1.1593	A_53_P103762
	118920642	*Ppp1r14d*	1.3373	A_53_P121243
	129300498	*Sirpa*	1.6381	A_53_P104495
	180129170	*Lama5*	1.7777	A_53_P134850
3	116956807	*Palmd*	1.2894	A_53_P156783
4	9469402	*Asph*	1.4916	A_53_P133679
	19482649	*Cpne3*	−1.0526	A_53_P150297
	35342545	*Mobkl2b*	1.2954	A_53_P167191
	111887133	*A030013N09Rik*	1.7994	A_53_P173459
	122370069	*Cap1*	−1.3924	A_53_P164318
5	82089821		−1.0199	A_53_P107809
	91325669	*Ankrd17*	−1.4014	A_53_P103987
6	41780689	*Pip*	−1.1330	A_53_P108514
	66469542	*Mad2l1*	−1.0849	A_53_P177517
	122854370	*Necap1*	−1.6767	A_53_P167918
7	48066915	*Mrgprb4*	−1.1216	A_53_P138268
	103571533		1.9850	A_53_P161168
	103802141	*Olfr631*	1.2903	A_53_P128993
	112226113	*Parva*	−1.0788	A_53_P146466
8	44634472	*Triml1*	2.8597	A_53_P127659
	74628670	*B3gnt3*	1.3186	A_53_P173754
	84885685	*Inpp4b*	1.5521	A_53_P107849
	87071779		2.0944	A_53_P112621
	108733780	*Cenpt*	1.0225	A_53_P125592
	109946820	*Nip7*	1.5030	A_53_P118435
9	32540264		−1.1423	A_53_P121033
	107273752	*Cacna2d2*	−1.2559	A_53_P150786
10	6945521	*Ppp1r14c*	−1.1874	A_53_P124781
	57843148	*Ranbp2*	−1.0838	A_53_P141256
	77396203	*Pfkl*	−1.0080	A_53_P106511
	89217026	*E030041M21Rik*	−1.4148	A_53_P140717
11	33639791	*Kcnip1*	−1.2893	A_53_P178993
	46470905	*Dppa1*	1.4241	A_53_P102723
	99865228	*Krt31*	−1.2697	A_53_P163547
	116570620	*St6galnac1*	−2.0574	A_53_P115288
	116570642	*St6galnac1*	−1.9370	A_53_P142502
	121532307	*Metrnl*	−1.0042	A_53_P105331
12	35635126	*Snx13*	1.1942	A_53_P146884
	41967094	*Immp2l*	−1.7377	A_53_P137343
	41987123	*Immp2l*	−1.2040	A_53_P128553
13	67940561	*C330011K17Rik*	1.1852	A_53_P106592
	70065745	*Srd5a1*	1.1006	A_53_P105119
	96540342	*Crhbp*	1.0787	A_53_P155927
	96808367	*Iqgap2*	1.4324	A_53_P117954
	101058907	*Mccc2*	−1.0261	A_53_P127939
	113886438		1.4000	A_53_P170982

Table 1. Continued.

Chromosome	Start position	Genes	DNA copy $\log_2$ ratio (BV-2/Normal)	Oligonucleotide No.*
17	6614146	*Vil2*	1.0930	A_53_P119030
	45026639	*Nfkbie*	1.1228	A_53_P152462
	78654120	*Heatr5b*	1.2652	A_53_P142376
	80076630	*Galm*	1.0117	A_53_P175435
18	43519207	*Dpysl3*	−1.0089	A_53_P162132
19	40994434	*Blnk*	1.3586	A_53_P145681
	44244501	*Pkd2l1*	1.0015	A_53_P135720
	44585311	*Sec31b*	1.0993	A_53_P174262

*Olionucleotide no. refers to the oligonucleotide identification number of Agilent mouse genome CGH microarray 44K.

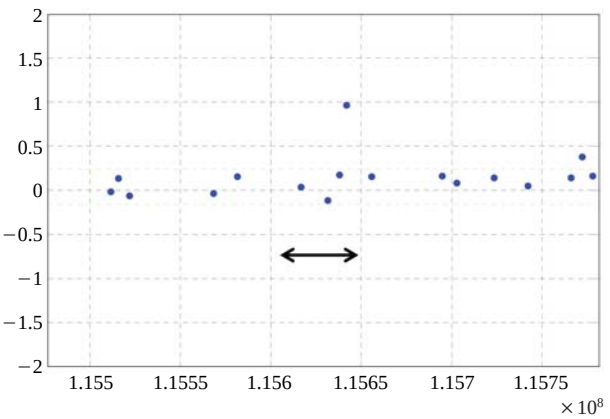

Figure 2. Profile of the $\log_2$ ratios near the *v-raf* viral oncogene 1 in chromosome 6. The arrow represents the genomic region of the *v-raf* viral oncogene 1 covered by four spots.

or loss segment if the neighbors of the gain spot have low ratios. This indicates that the segmentation gives more useful information for detection of long-range aberration than for single spot.

Confirmation of Gain and Loss by Polymer Chain Reaction

We PCR-amplified four genomic regions to test the reliability of the oaCGH data. As the $\log_2$ ratio of a single oligonucleotide (spot) provides a representative value for the covering genomic region, we assumed that the genomic region between two adjacent spots might have the average $\log_2$ ratio of these two spots. The PCR regions were selected based on the $\log_2$ ratio of the nearest spots on either side of the segment. For the confirmation of gained regions, two regions of chromosome 4 were used as templates, one region for a gain control and one region for a gain test reaction (Table 3). The quantity of PCR product derived from BV-2 genomic DNA in the gain test region was much greater than that obtained from normal mouse genomic DNA while the quantity of the PCR products in the gain control region were the same in both BV-2 DNA and normal mouse DNA (Figure 4(A)). A similar approach was applied to a loss control region and loss test region in chromosome 8. The quantity of PCR product obtained from BV-2 genomic DNA in the loss test region was much less than that obtained from normal mouse genomic DNA and the quantity of PCR product from BV-2 DNA in the loss control region was exactly the same as that from normal DNA (Figure 4(B)). The PCR results from both the gain and loss regions shows a good agreement with the oaCGH results and with our assumption that the quantity of PCR product is proportional to the copy number of the template DNA.

Taken together, the segmentation analysis of the oaCGH data successfully revealed segments with chromosomal imbalances (losses and gains) as detected by BV-2/normal hybridization (Figure 3 and Table 2). The total size of each gain and loss segment was 64.0 Mb and 253.5 Mb, respectively. This suggests that BV-2 cells might have experienced more events of loss than gain for its immortalization.

Conclusions

BV2 microglial cells show great potential as a useful research model not only for studies of microglial biology but also for research on various CNS diseases such as neurodegenerative diseases in which microglial activation is prominent in the pathophysiology. However, alterations of DNA copy number in BV-2 cells may cause modifications in gene expression levels and functions, which may results in different biological properties from normal microglial cells. Therefore, pathophysiological and drug development studies in BV-2 cells might require cautious elucidation and further study taking genome variations into consideration. Data derived from oaCGH analysis might con-

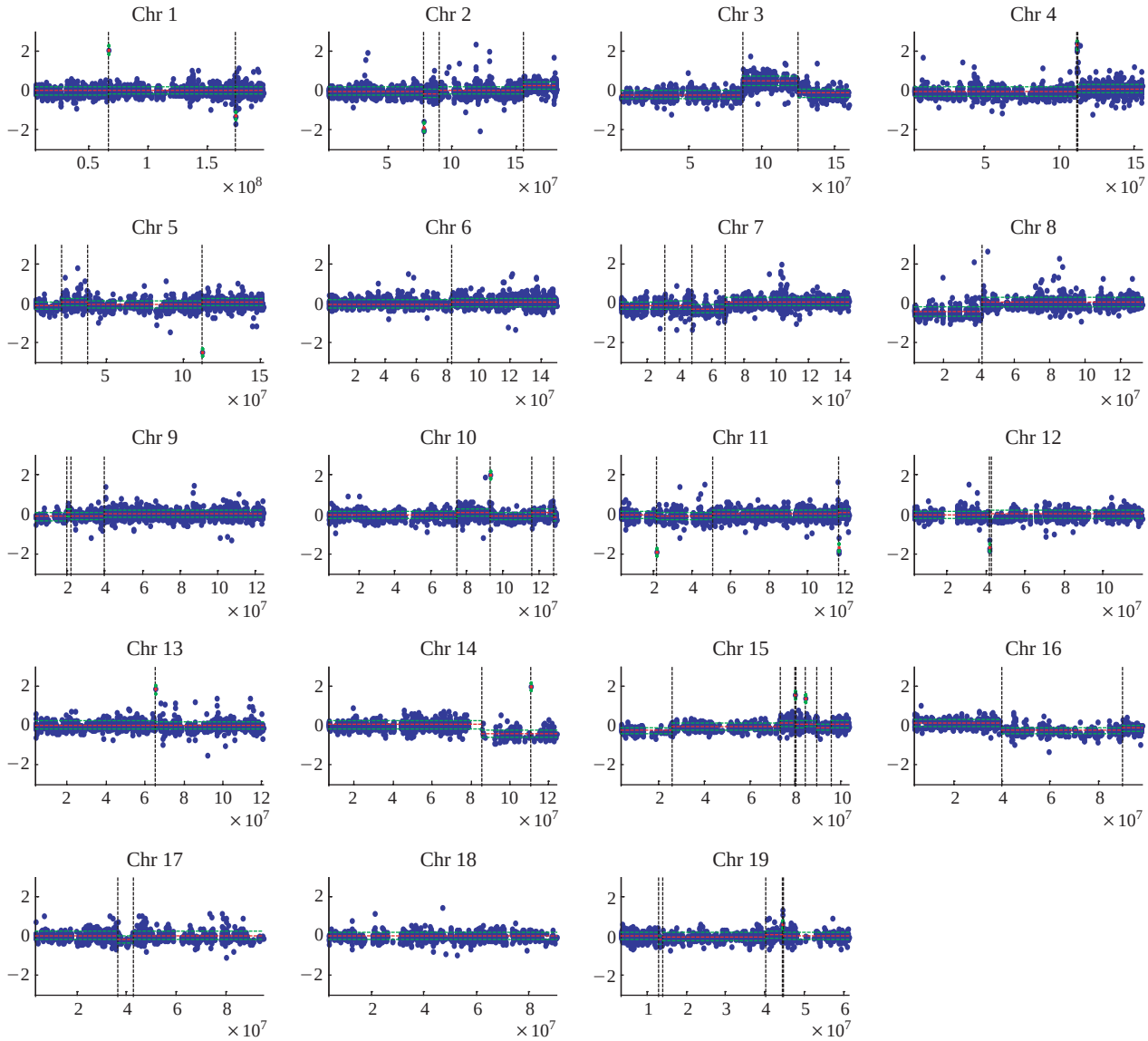

Figure 3. Graphical representation of the oaCGH profile and segmentation results.

tribute to an increased understanding of BV-2 microglial cells and the characteristics of microglia, and microglia-associated pathologies.

Materials and Methods

Cell Culture and DNA Extraction

BV-2 cells (a mouse microglial cell line) were originally developed by Dr. V. Bocchini at the University of Perugia (Perugia, Italy)[3], and were provided by Dr. K. Suk at Kyungpook National University (Daegu, Korea). The cell line was cultured in Dulbecco's Modified Eagle's Medium (DMEM) supplemented with 5% fetal bovine serum (FBS) and 50 μg/mL of gentamicin, and maintained in a humidified incubator with 5% CO_2. Genomic DNA was extracted as described previously[12].

Genomic DNA Labeling and Hybridization to Oligonucleotide Microarray

For each CGH hybridization, 20 ng of genomic DNA from the reference mouse genomic DNA sample (Cat.#G3091, Promega, Madison, WI) and the BV2 genomic DNA preparation were amplified with the GenomePlex whole-genome amplification kit accord-

Table 2. Segmentation analysis of oaCGH data using the CGH segmentation method [13]. The aberrant segment ($|\mu_k| > \sigma$) was marked in bold.

Chromosome	Start of segment	End of segment	Size of segment (bp)	μ_k	σ
1	4336501	66711188	62374688	−0.0291	0.1928
	66745542	173300670	106555129	0.0166	
	173340158	**173400547**	**60390**	**− 1.2734**	
	173410499	196871918	23461420	0.0162	
2	3104269	77470986	74366718	−0.0306	0.2065
	77702452	**77792980**	**90529**	**− 1.8721**	
	78022581	90203992	12181412	−0.1636	
	90292975	155798002	65505028	−0.0039	
	155815152	**181797594**	**25982443**	**0.2368**	
3	**3445973**	**86952997**	**83507025**	**− 0.2207**	0.2193
	87075657	**124604754**	**37529098**	**0.4855**	
	125482986	159870361	34387376	−0.1383	
4	3377972	111570775	108192804	−0.0635	0.2217
	111634766	**111955477**	**320712**	**2.3402**	
	112125091	155029035	42903945	0.0748	
5	3285647	20217443	16931797	−0.1124	0.1914
	20276086	37351205	17075120	0.0517	
	37389988	111839975	74449988	−0.0525	
	111974568	151918350	39943783	0.0449	
6	3274714	82671889	79397176	−0.0418	0.1989
	82713786	149512282	66798497	0.034	
7	3215773	30756174	27540402	−0.1221	0.2065
	30773305	47366242	16592938	−0.1027	
	47390541	**68479871**	**21089331**	**− 0.2902**	
	68493479	145131356	76637878	0.0869	
8	**3151837**	**41176875**	**38025039**	**− 0.4286**	0.2344
	41703055	132061985	90358931	0.0799	
9	3156654	20036818	16880165	−0.1177	0.1844
	20050630	22222180	2171551	0.0924	
	22241209	39877685	17636477	−0.0964	
	39877898	123957580	84079683	0.0293	
10	3051921	74415958	71364038	−0.0377	0.1791
	74421828	93039509	18617682	0.0937	
	93170824	116323217	23152394	−0.0949	
	116352687	128393696	12041010	0.0645	
	128476277	129759313	1283037	−0.1666	
11	3100146	21686705	18586560	−0.0301	0.1817
	21888515	51115343	29226829	−0.074	
	51163251	116510176	65346926	0.0123	
	116590032	121652628	5062597	0.0686	
12	3238250	41698532	38460283	−0.0132	0.1862
	41967094	**41987182**	**20089**	**− 1.628**	
	42836142	119905084	77068943	0.0002	
13	3489596	64937786	61448191	0.0088	0.2071
	65101857	120604804	55502948	−0.0022	
14	6628547	85476200	78847654	0.0323	0.1867
	85666700	**109719813**	**24053114**	**− 0.4325**	
	110564578	**123875911**	**13311334**	**− 0.4103**	
15	**3229082**	**25671269**	**22442188**	**− 0.2674**	0.1621
	25741766	73222004	47480239	−0.0519	
	73317114	80027716	6710603	0.0988	
	80071486	84383741	4312256	0.0564	
	84499017	89301252	4802236	0.0885	
	89303290	95597650	6294361	−0.0912	
	95617883	103393076	7775194	0.0594	

Table 2. Continued.

Chromosome	Start of segment	End of segment	Size of segment (bp)	μ_k	σ
16	3508254	39019253	35511000	0.135	0.1683
	40062253	**90015523**	**49953271**	**−0.2708**	
	90049958	98114503	8064546	−0.1454	
17	3075728	36655848	33580121	0.024	0.2056
	36681599	42938440	6256842	−0.1821	
	42951661	95077557	52125897	0.014	
18	3254025	90727455	87473431	−0.005	0.1893
19	3259856	12929431	9669576	0.0179	0.1936
	12951500	**13913235**	**961736**	**−0.2027**	
	13937881	40218756	26280876	−0.0397	
	40299177	44387843	4088667	0.0617	
	44398741	**44585370**	**186630**	**0.6016**	
	44607754	61288400	16680647	0.015	

Table 3. PCR conditions for the amplification of four genomic regions. The control region was selected from the same chromosome to which the test region belongs and each PCR reaction was carried out against both BV-2 genomic DNA and normal mouse genomic DNA.

		Primer sequence (5′→3′)	Genomic region covered (*)	Size of PCR product (bp)	Annealing temperature (°C)	Cycles
Gain control	Forward	caggcagggctacacagaga	chr4 : 11137387-11140387 (0.02)	365	55	30
	Reverse	caaaaccctgcagccataga				
Gain test	Forward	accgctttttcctttcaagc	chr4 : 112634336-112637336 (0.765)	302	55	30
	Reverse	aggccaaatgcttcattcct				
Loss control	Forward	aaggctagcggatttcttgc	ch8 : 60662691-60665691 (0.02)	1031	60	27
	Reverse	ccccacaaagctgctcacta				
Loss test	Forward	tgtgggtgtgggctttaaga	ch8 : 31358126-31361126 (−0.515)	1232	60	27
	Reverse	aggttggaacaggagggatg				

(*) The genomic location was based on the mouse genome database (UCSC mm8, NCBI Build 36) and the value in parentheses represents the average $\log_2$ ratio of the nearest two spots to the PCR region.

ing to the supplier's protocols (Sigma). Briefly, the random fragmentation step was performed by incubating a mixture of 10X fragmentation buffer and genomic DNA at 94˚C for exactly 4 minutes. The fragmented samples were immediately cooled on ice. For OmniPlex library preparation, the fragmented samples were mixed with 1X library buffer and library stabilization solution and then heated at 95˚C for 2 min. Library preparation enzyme was added to the samples and they were placed in a thermal cycler and incubated as follows; 16˚C for 20 min, 24˚C for 20 min, 37˚C for 20 min, 75˚C for 5 min, and finally 4˚C hold. The whole-genome amplification (WGA) reaction was carried out in a volume of 20 μL with 15 μL the OmniPlex library sample, 7.5 μL of 10X amplification master mix and 12.5 units of WGA DNA polymerase. Amplification conditions were as follows: initial denaturation at 95˚C for 3 min, 14 cycles of 95˚C for 15 sec and 65˚C for 5 min, and hold at 4˚C. The amplified samples were purified using the QIAQuick PCR clean-up kit (QIAGEN). Labeling reactions were performed with 5 μg of purified, amplified DNA and a Bioprime labeling kit (Invitrogen) according to the manufacturer's instructions in a volume of 50 μL with a modified dNTP pool containing 120 μM each of dATP, dGTP, and dCTP; 60 μM dTTP; and 60 μM Cy5-dUTP or 60 μM Cy3-dUTP for the sample labeling. We conducted a dye-swap experiment to compensate dye bias. Labeled targets were subsequently purified using the QIAQuick PCR clean-up kit (QIAGEN). After checking the labeling efficiency, Cy3-labeled and Cy5-labeled DNA targets were mixed and 10X blocking solution, 2X hybridization buffer and human Cot-1 DNA (Applied Genetics, USA) were added. The samples were incubated at 95˚C for 5 min followed by 37˚C for 30 min. The labeled targets were directly pipetted onto an assembled mouse genome CGH microarray 44K (Agilent Technologies) containing *in situ* synthe-

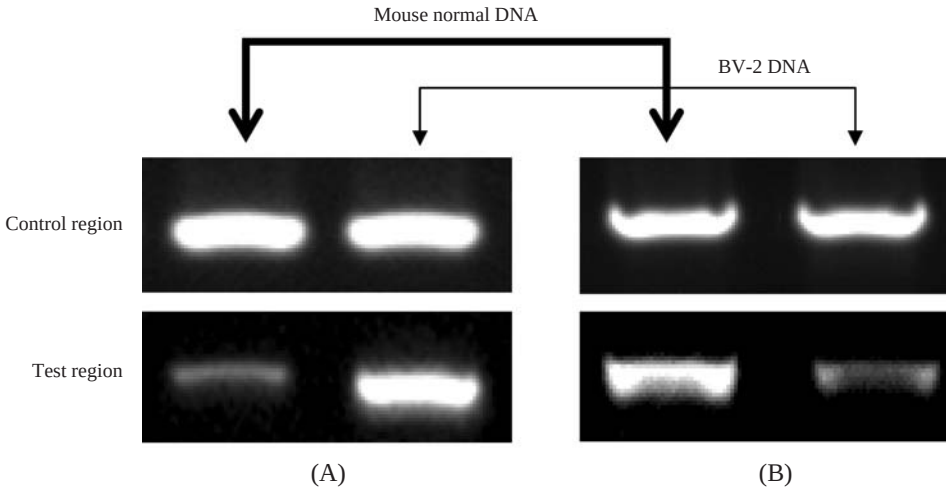

Figure 4. Comparison of PCR product quantities for four genomic regions in BV-2 DNA and normal mouse DNA examined by gel electrophoresis. (A) gain control (upper) and gain test (lower) (B) loss control (upper) and loss test (lower).

sized 60-mer oligonucleotides for 43,000+ coding and noncoding mouse sequences based on the UCSC mmu5 mouse genome database (NCBI build 33, May 2004). The arrays were hybridized at 65°C for 40 hours using an Agilent Hybridization oven (Agilent Technologies). The hybridized microarrays were washed according to the manufacturer's washing protocol (Agilent Technologies).

Image and Data Analysis

Micorarry slide images were obtained by a GenePix 4200A laser scanner (Axon Instruments, Foster City, CA) and were saved in a GenePix Result (GPR) format. The array data were first normalized by averaging ratios from dye-swapped hybridizations and then re-normalized by the intensity-dependent "lowess normalization" method in GeneSpring 7.2 (Agilent, Palo Alto, CA). Briefly, the GPR files were imported into GeneSpring 7.2 (Agilent, Palo Alto, CA) and were normalized by the intensity-dependent "lowess normalization" method. The value of $\log_2$ (Cy5/Cy3) should theoretically be -1 for a single loss, 0 for the normal state, 0.585 for a single gain when BV-2 DNA and reference DNA are labeled by Cy5 and Cy3, respectively. In practice, microarray experiments are subject to sources of variation which create noise and bias the theoretical values. The average for two replicate arrays was further determined. The sex chromosomes X and Y are excluded in our analysis because the reference genomic DNA was a mixture of male and female genomic DNA. We first conducted single *t*-tests against the oaCGH data with a cross-gene error model function in GeneSpring 7.2 to identify spots having significantly different values from the $\log_2$ ratio of 0. The cross-gene error model assumes that the amount of variability is a function of the control strength (Cy3 signal in this study) with all the measurements for a single experimental condition. This function makes it possible to evaluate where the $\log_2$ ratio of each spot is significantly different from 0 even for single oaCGH data. In addition, we also analyzed oaCGH data with the CGH segmentation method[13] to access the status of each array element (spot) in the context of its neighbors because the oaCGH profile can be viewed as a succession of segments that represent homogeneous regions in the genome whose oligonucleotides share the same relative copy number on average. The CGH-segmentation method, like other segmentation methods, considers the normalized ratio for each spot in a microarray as a realization of a Gaussian process whose parameters are affected by an unknown number of abrupt changes at unknown locations on the genome. As the number of segment numbers, k, is usually unknown, it is estimated by the maximization of the penalized log-likelihood $\tilde{L}_k$ as shown below:

$$\tilde{L}_k = \hat{L}_k - \beta \cdot 2k, \hat{k} = Arg\max_k(\tilde{L}_k)$$

where $\hat{L}_k$, β and $\hat{k}$ are the maximum of log-likelihood L_k, a constant of penalization and the estimated number of segments, respectively. The value of β is chosen adaptively. We assume a Gaussian distribution $N(\mu_k, \sigma^2)$ for each segment k, which consists of $\log_2$ ratios, ϕ_i's, where ϕ_i is the $\log_2$ ratio of the i^{th} spot in a microarray. The segmentations are applied for each chromosome separately and all segments within a chromosome are assumed to have the same variance of σ^2. The log-likelihood can be decomposed into a sum of local likelihoods calculated on each segment[13]:

$$L_k = \sum_{k=1}^{K} l_k$$

where $l_k = -\frac{1}{2}\sum_{i=i_{k-1}+1}^{i_k}\left[\log(2\pi\times\sigma^2)+\left(\frac{\phi_i-\mu_k}{\sigma}\right)^2\right]$

The mean μ_k for each segment and the variance σ are calculated using maximum likelihood:

$$\hat{\mu}_k=\frac{1}{i_k-i_{k-1}}\sum_{i=i_{k-1}+1}^{i_k}\theta_i,\ \hat{\sigma}^2=\frac{1}{n}\sum_{k=1}^{k}\sum_{i=i_{k-1}+1}^{i_k}(\phi_i-\hat{\mu}_k)^2$$

Where n is the total number of oligonucleotides. The chromosomal location for each segment was based on the mouse genome database (UCSC mm8, NCBI Build 36).

Validation of Copy Number Changes from oaCGH Data by Polymerase Chain Reaction

To test the reliability of oaCGH data, we carried out polymerase chain reactions against four genomic regions with both genomic DNA samples isolated from BV2 cells and from reference mice. The primer sequences and genomic regions are shown in Table 3. PCRs were performed in a total volume of 20 μL of ExTaq™ (Takara, Japan) with 100 ng of the genomic DNA samples, a final concentration of 10 pmoles/μL oligonucleotide primers. The reference mouse genomic DNA was the same as that used in the oaCGH experiment (Cat.#G3091, Promega, Madison, WI). The cycle number of the PCRs was selected to be between the mid-exponential phase and the late-exponential phase increase in DNA copy number. The thermal cycling conditions of the PCRs were as follows: gain control and gain test, 30 cycles of denaturation at 98 ˚C for 10 s, annealing at 55˚C for 30 s, and extension at 72˚ C for 60 s; loss control and loss test, 27 cycles of denaturation at 98˚C for 10 s, annealing at 60˚C for 30 s, and extension at 72˚C for 60 s.

Acknowledgements

This research was financially supported by the Ministry of Education, Science Technology (MEST) and Korea Industrial Technology Foundation (KOTEF) through the Human Resource Training Project for Regional Innovation, and also by the Basic Research Program (R01-2006-000-10314-0) of the Korea Science & Engineering Foundation.

References

1. Streit, J.W. Microglia as neuroprotective, immunocompetent cells of the CNS. *Glia.* **40**, 133-139 (2002).
2. Kim, S.U. & Vellis, J. de. Microglia in health and disease. *J. Neurosci. Res.* **81**, 302-313 (2005).
3. Blasi, E., Barluzzi, R., Bocchini, V., Mazzolla, R. & Bistoni, F. Immortalization of murine microglia cells by *v-raf/v-myc* carrying retrovirus. *J. Neuroimunol.* **27**, 229-237 (1990).
4. Albright, A.V. & González-Scarano, F. Microarray analysis of activated mixed glial (microglia) and monocyte-derived macrophage gene expression. *J. Neuroimmunol.* **157**, 27-38 (2004).
5. Bocchini, V. *et al.* An immortalized cell line expresses properties of activated microglial cells. *J. Neurosci. Res.* **31**, 616-621 (1992).
6. Gebicke-Haerter, P.J. Microarrays and expression profiling in microglia research and in inflammatory brain disorders. *J. Neurosci. Res.* **81**, 327-341 (2005).
7. Mrak, R.E. & Griffin, W.S.T. Glia and their cytokines in progression of neurodegeneration. *Neurobiol. Aging* **26**, 349-354 (2005).
8. Zierler, S. *et al.* Ultraviolet irradiation-induced apoptosis does not trigger nuclear fragmentation but translocation of chromatin from nucleus into cytoplasm in the microglial cell-line, BV-2. *Brain Res.* **1121**, 12-21 (2006).
9. Kallioniemi, A. *et al.* Comparative genomic hybridization for molecular cytogenetic analysis of solid tumors. *Science* **259**, 818-821 (1992).
10. Ylstra, B. *et al.* BAC to the future! or oligonucleotides: a perspective for micro array comparative genomic hybridization (array CGH). *Nucleic Acids. Res.* **34**, 445-450 (2006).
11. Pinkel, D. & Albertson, D.G. Array comparative genomic hybridization and its applications in cancer. *Nat. Genet.* **37**(Suppl), S11-17 (2005).
12. Do, J.H., Kim, I.S., Park, T.K. & Choi, D.K. Genome-wide examination of chromosomal aberrations in neuroblastoma SH-SY5Y cells by array-based comparative genomic hybridization. *Mol. Cells* **24**, 105-112 (2007).
13. Picard, F., Robin, S., Lavielle, M., Vaisse, C. & Daudin, J.J. A statistical approach for array CGH analysis. *BMC Bioinformatics* **6**, 27 (2005).
14. Rocke, D.M. & Durbin, B. A model for measurement errors for gene expression arrays. *J. Comput. Biol.* **8**, 557-569 (2001).